

A Single-Molecule Perspective on the Role of Solvent Hydrogen Bonds in Protein Folding and Chemical Reactions

Lorna Dougan,^{*,[a]} Ainavarapu Sri Rama Koti,^[b] Georgi Genchev,^[c] Hui Lu,^[c] and Julio M. Fernandez^{*,[a]}

We present an array of force spectroscopy experiments that aim to identify the role of solvent hydrogen bonds in protein folding and chemical reactions at the single-molecule level. In our experiments we control the strength of hydrogen bonds in the solvent environment by substituting water (H₂O) with deuterium oxide (D₂O). Using a combination of force protocols, we demonstrate that protein unfolding, protein collapse, protein folding and a chemical reaction are affected in different ways by substituting H₂O with D₂O. We find that D₂O molecules form an integral part of the unfolding transition structure of the immunoglobulin

module of human cardiac titin, I27. Strikingly, we find that D₂O is a worse solvent than H₂O for the protein I27, in direct contrast with the behaviour of simple hydrocarbons. We measure the effect of substituting H₂O with D₂O on the force dependent rate of reduction of a disulphide bond engineered within a single protein. Altogether, these experiments provide new information on the nature of the underlying interactions in protein folding and chemical reactions and demonstrate the power of single-molecule techniques to identify the changes induced by a small change in hydrogen bond strength.

1. Introduction

The structure and dynamics of proteins and enzymatic activity is intrinsically linked to the strength and positions of hydrogen bonds in the system.^[1] A hydrogen bond results from an attractive force between an electronegative atom and a hydrogen atom.^[2] The hydrogen is attached to a strongly electronegative heteroatom, such as oxygen or nitrogen, termed the hydrogen-bond donor. This electronegative atom decentralizes the electron cloud around the hydrogen nucleus, leaving the hydrogen atom with a positive partial charge. Since the hydrogen atom is smaller than other atoms, the resulting partial charge represents a large charge density. A hydrogen bond results when this strong positive charge density attracts a lone pair of electrons on another heteroatom, which becomes the hydrogen-bond acceptor. Although stronger than most other intermolecular forces, the hydrogen bond is much weaker than both the ionic and the covalent bonds.^[2] Within macromolecules such as proteins and nucleic acids, it can exist between two parts of the same molecule, and provides an important constraint on the molecule's overall shape.^[3] The hydrogen bond was first introduced in 1912 by Moore and Winmill^[4] and its importance in protein structure was first made apparent in the 1950s by Pauling^[5–7] and in the early treatise of Pimental & McClellan.^[8] More recently, detailed structural patterns of hydrogen bonding have been analyzed using techniques such as X-ray diffraction to identify recurrent properties in proteins.^[9] Along with its importance in protein structure, the relative strength of hydrogen bonding interactions is thought to determine protein folding dynamics.^[1,10] The breaking and reformation of hydrogen bonds within the protein and with the solvent environment is therefore a key determinant of protein dynamics.^[11] In solution, hydrogen bonds are not rigid, but rather

fluxional on a timescale of ~50 ps.^[12] This fluxional behaviour is due to the low activation energy of hydrogen bond rupture ~1–1.5 kcal mol⁻¹. Indeed, in the absence of water considerably higher activation energies have been calculated and it has been proposed that diminished fluxional motions would not support many life processes, since physiological temperatures could not lead to rupture and realignment of hydrogen bonds.^[12]

One model system for exploring the structure and dynamics of hydrogen bonds is that of water (H₂O) and heavy water, deuterium oxide (D₂O).^[13] The oxygen atom of a water molecule has two lone pairs, each of which can form a hydrogen bond with hydrogen atoms on two other water molecules. This arrangement allows water molecules to form hydrogen bonds with four other molecules.^[14] On the macroscopic level, both experimental^[15] and theoretical studies^[16] studies have demonstrated that in water, deuterium bonds are stronger than hydrogen bonds by ~0.1 to 0.2 kcal mol⁻¹. The increased strength of the deuterium bond is attributed to the higher

[a] Dr. L. Dougan, Prof. J. M. Fernandez
Biological Sciences, Columbia University
New York, 10027 (USA)
Fax: (+1) 212-854-9474
E-mail: ldougan@biology.columbia.edu
jfernandez@columbia.edu

[b] Dr. A. S. R. Koti
Department of Chemical Sciences
Tata Institute of Fundamental Research
Mumbai 40005 (India)

[c] G. Genchev, Prof. H. Lu
Department of Bioengineering
University of Illinois, Chicago 60607 (USA)

mass of the deuteron atom lowering the zero-point vibrational energy of the intermolecular mode of highest frequency. This mode is associated with the bending motion of the proton donor molecule distorting the linearity of the hydrogen bond.^[16] Although the increase in bond strength is small for individual bonds, the cumulative effect on a large molecule in solution may be significant. Indeed, a large number of studies have explored how intramolecular and hydration interactions are affected when the solvent environment is changed from H₂O to D₂O. Several experiments have found that, in the case of simple hydrocarbons and noble gases, D₂O is a better solvent than H₂O.^[17–20] In these studies the hydrophobic effect, as measured by hydrocarbon solubility, was considered to be less pronounced in D₂O than H₂O. These observations were surprising given that hydrogen bonds in D₂O are stronger than hydrogen bonds in H₂O^[15,16] and it might be expected that a more strongly associating fluid^[13] would exhibit a more pronounced hydrophobic effect, contrary to what is observed.^[17–20] A number of theoretical studies have also investigated the influence of D₂O on the hydration of simple hydrocarbons.^[21–23] Indeed, this model system is often explored in an attempt to understand the characteristics of hydrophobic hydration and interaction.^[21] However, the experimental and computational observation that D₂O is a better solvent than H₂O for hydrocarbons is in direct contrast to the behaviour of proteins and larger macromolecules in these solvent environments. Experiments have found D₂O is a worse solvent than H₂O and that polypeptides tend to reduce their surface area in contact with the solvent by adopting more compact globular shapes or associating into larger aggregates. This has been inferred mainly from the stabilizing effect of D₂O on the thermal denaturation of several proteins, as induced by guanidinium chloride and urea^[17,24,25] and from the promotion of aggregated states of oligomeric proteins.^[26–28] In a number of cases,^[25,27] the stabilizing effect of D₂O has been attributed to the enhancement of hydrophobic interactions. However, the influence of D₂O on the thermodynamic stability of proteins is not general, as some proteins are less stable in D₂O than in H₂O at room temperature.^[29–31] Clearly then, the intramolecular and hydration interactions of proteins in D₂O are distinct from that of simple systems such as hydrocarbons. While there have been many breakthroughs in understanding the behaviour of hydrocarbons in D₂O, it is apparent that the proposed theoretical models for these simple systems require modification when discussed in the context of hydrophobic effects in protein stability and folding. In particular with proteins, whose folded structure is the result of a delicate balance between intramolecular and hydration interactions, D₂O may alter the dynamics of protein function in subtle and non-intuitive ways.^[32–35] Interestingly, in contrast to the wealth of thermodynamic data on the influence of D₂O on hydrocarbon solvation and protein stability, little is known about the effects of D₂O on the dynamics of protein folding.^[36] Knowledge of the influence of D₂O on the conformational dynamics of a protein may be important both at a basic level, to identify the nature of the underlying interactions in protein folding, and also for its possible implications on the catalytic efficiency of enzymatic proteins in this

medium. Indeed, what is still lacking is a molecular level understanding of the influence of solvent hydrogen bonding strength on protein folding dynamics.

Herein, we take a single-molecule approach to explore the role of solvent hydrogen bonding and hydrogen bond strength on protein folding and a chemical reaction. We utilize force spectroscopy techniques to apply a denaturing force along a well-defined reaction coordinate driving proteins to a fully extended unfolded state.^[37] This level of experimental control allows statistical examination of the unfolding and folding pathways of a protein^[38–42] and a chemical reaction^[43] in the solvent environment of interest. Perturbing the equilibrium conformation of a single protein using mechanical forces has become a powerful tool to study the details of the underlying folding free energy landscape. Along the unfolding pathway of the protein, a mechanically resistant transition state determines the force-dependent rate of unfolding, $k_u(F)$.^[44] The unfolding transition state is characterized by two parameters: the size of its activation energy, ΔG_{ur} , and the elongation of the protein necessary to reach the transition state, Δx_u .^[39,45] Of particular interest are the force spectroscopy measurements of Δx_u , which provide a direct measure of the length scales of a transition state. For example, for protein unfolding, Δx_u is in the range of 1.7–2.5 Å.^[37,46] These values of Δx_u are comparable to the size of a water molecule, suggesting that water molecules, and thus hydrogen bonds, are integral components of the unfolding transition state of a protein.^[39] In addition to exploring the role of solvent molecules in the unfolding transition state of a protein, force spectroscopy provides access to the collapse trajectories of individual proteins. Indeed, using these techniques, it becomes possible to explore the role of the solvent environment in protein collapse^[42] and the dynamics of protein folding.^[47] Therefore, in order to determine the role of solvent hydrogen bonds and hydrogen bond strength in protein folding, we use single-molecule force spectroscopy to measure the force-dependent properties of the I27 immunoglobulin module of human cardiac titin in the presence of H₂O and D₂O.

In addition to exploring protein folding, single-molecule force spectroscopy has recently emerged as a powerful new tool to directly measure the effect of a mechanical force on the kinetics of chemical reactions. A recent review by Beyer and Clausen-Schaumann describes the role of mechanical forces in catalyzing chemical reactions.^[48] The authors noted that a general problem in previous studies was that the reaction of interest could never be oriented consistently with respect to the applied mechanical force and thus, the effect of mechanical forces on these chemical reactions could not be studied quantitatively. Force-clamp spectroscopy has overcome these barriers to directly measure the effect of a mechanical force on the kinetics of a chemical reaction.^[43,44,49] In these experiments, a disulfide bond is engineered into a well-defined position within the structure of the protein I27. Disulfide bonds are covalent linkages formed between thiol groups of cysteine residues. These bonds are common in many extracellular proteins and are important both for mechanical and thermodynamic stability. The reduction of these bonds by other

thiol-containing compounds via an uncomplicated S_N2 -type mechanism^[44] is common both *in vivo* and *in vitro*; a commonly used agent is the dithiol reducing agent dithiothreitol (DTT). To directly probe the role of the solvent hydrogen-bond strength on a chemical reaction, we measure the rate of disulfide bond reduction in the presence of the reducing agents DTT and tris(2-carboxyethyl)phosphine (TCEP) in D_2O solution.

2. Results and Discussion

2.1. A Mechanical Fingerprint for Protein Unfolding

Using molecular biology techniques, we engineered tandem modular proteins that consist of identical repeats of a protein of interest.^[50] For this study, we constructed polyproteins with eight repeats of the human cardiac titin domain I27.^[51] The I27₈ polyprotein is ideal for these experiments as its mechanical properties have been well characterized both experimentally^[39,46,50,52,53] and *in silico*, using molecular dynamics techniques.^[54–56] When a polyprotein is extended by atomic force microscopy (AFM, Figure 1a), its force properties are unique

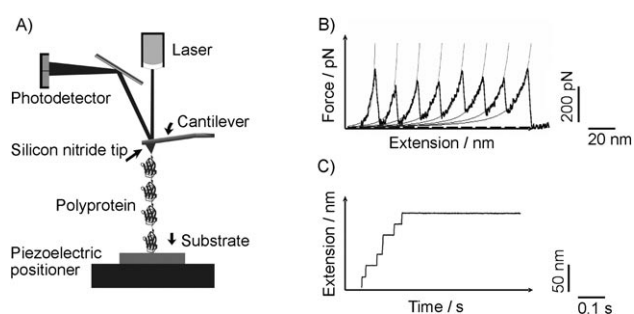


Figure 1. A) Simplified diagram of the atomic force microscope showing the laser beam reflecting on the cantilever, and over to a photodiode detector. The photodiode signal is calibrated in picoNewtons. When pressed against the layer of protein attached to a substrate, the cantilever tip can adsorb a single protein molecule. Extension of a molecule by retraction of the piezoelectric positioner results in deflection of the cantilever. B) When a polyprotein is pulled at constant velocity by means of a piezoelectric actuator the increasing pulling force triggers the unfolding of a module. Continued pulling repeats the cycle resulting in a force-extension curve with a characteristic “sawtooth pattern”. C) When pulling is done under feedback, the piezoelectric actuator abruptly adjusts the extension of the polyprotein to keep the pulling force at a constant value (force-clamp). Unfolding now results in a staircase-like elongation of the protein as a function of time.

mechanical fingerprints that unambiguously distinguish them from the more frequent non-specific events.^[46] The AFM is operated in two distinct modes. The first is known as the force–extension mode,^[50] where the pulling velocity is kept constant, resulting in a force versus extension trace with a characteristic sawtooth pattern (Figure 1B). The second mode is known as force–clamp,^[37] where the pulling force is kept constant with time, resulting in an extension versus time trace with a characteristic staircase pattern (Figure 1C).

2.2. Force-Extension Experiments Measure the Rupture Force of I27 in D_2O

The strength of multiple parallel hydrogen bonds have been studied extensively, using both theoretical and statistical mechanical approaches, as well as experimentally with AFM.^[57–62] These noncovalent bonds are indispensable to biological function, where they play a key role in cell adhesion and motility, formation and stability of proteins structures and receptor–ligand interactions.^[3] To further explore the role of solvent hydrogen bonding in the unfolding process, we completed force–extension experiments on the protein I27 in H_2O and D_2O . In these experiments, a polyprotein is extended by retracting the sample-holding substrate away from the cantilever tip at a constant velocity of 400 nm s^{-1} . As the protein extends, the pulling force rises rapidly, causing the unfolding of one of the I27 modules in the chain. Unfolding then extends the overall length of the protein, relaxing the pulling force to a low value. As the slack in the length is removed by further extension, this process is repeated for each module in the chain resulting in force vs extension trace with a characteristic sawtooth pattern appearance. Figure 2A shows a typical force extension trace for unfolding the protein I27 in D_2O . Figure 2C shows a histogram of peak unfolding forces, F_{unfold} obtained from the sawtooth patterns’ traces ($N=150$) like those in Figure 2A. It is apparent that when the solvent environment is changed from H_2O to D_2O , F_{unfold} increases from 204 pN to 240 pN. Inspection of all force extension curves reveals that many of the force extension curves deviate from the expected entropic elasticity, revealing a pronounced hump that tends to disappear on unfolding of all the modules (Figure 2B). This

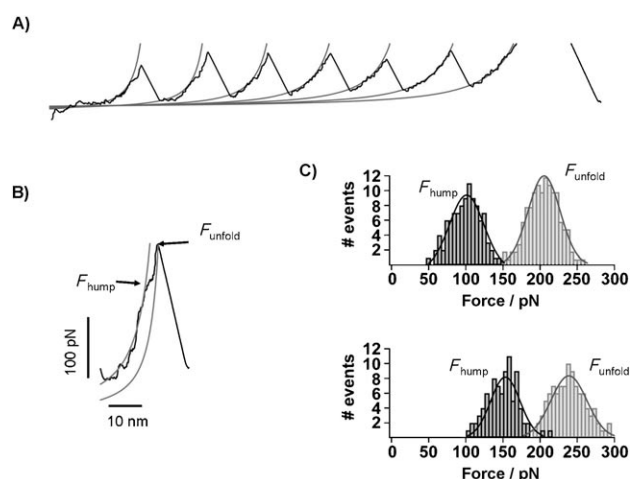


Figure 2. A) Force-extension relationship for the polyprotein (I27)₈, constructed from tandem repeats of the I27 module, in D_2O , showing a prominent hump in the rising phase of the initial force peaks which cannot be fitted with the worm-like chain (WLC) model (thin lines). B) The hump begins at a force, F_{hump} , that is smaller than the force required to unfold the module completely, F_{unfold} . The thin lines are fits of the WLC model to the data before and after the hump. C) Histogram of F_{hump} and F_{unfold} in H_2O (top) and D_2O (bottom). Gaussian fits (—) to the data give average values of $F_{\text{hump}} = 105 \text{ pN}$ and $F_{\text{unfold}} = 204 \text{ pN}$ ($N=100$) for H_2O , while in the case of D_2O $F_{\text{hump}} = 150 \text{ pN}$ and $F_{\text{unfold}} = 240 \text{ pN}$ ($N=100$). The pulling speed is 400 nm s^{-1} .

hump is observed when unfolding the protein I27 both in H₂O^[53] and D₂O and begins at a force, F_{hump} , that is smaller than the force required to completely unfold the module, F_{unfold} . Previously, steered molecular dynamics (SMD) simulations have shown that for I27 rupture of a pair of hydrogen bonds in the A and B β -strands near the amino terminus of the protein domain causes an initial extension of the protein, before the unfolding transition state is reached.^[53] The hump observed both in the force-extension experiments and in SMD simulations was attributed to an unfolding intermediate in the protein. Disruption of the relevant hydrogen bonds in the A and B β -strands protein by site-directed mutagenesis eliminated this unfolding intermediate.^[53] On close inspection of all force-extension traces, it is found that the hump is present at higher forces in D₂O (around 150 pN) than in H₂O (around 105 pN), F_{hump} in Figure 2C. Therefore, an increase in solvent hydrogen bond strength of ~ 0.1 to 0.2 kcal mol⁻¹ yields an increase in both F_{unfold} and F_{hump} for I27. Interestingly, a recent model has proposed that the critical force for bond rupture in a protein is dependent on the dissociation strength of hydrogen bonds in the system, which vary depending on the solvent conditions.^[60] In this model, an increase in hydrogen-bond strength of 0.2 kcal mol⁻¹, as is the case for D₂O as compared with H₂O, would yield an increase in the rupture force of $\sim 30\%$.^[60] This is in remarkable agreement with the increase in force we observe for I27 when the solvent is changed from H₂O to D₂O, namely F_{unfold} (20%) and F_{hump} (40%).

Interestingly, while both the folded protein and the intermediate are stabilized in the presence of D₂O, the stabilization is greater for the intermediate (40%). This enhanced stabilization suggests that D₂O plays a key role in the unfolding transition state of the I27 intermediate. Furthermore, while we make the assumption that hydrogen and deuterium are not exchanging with the protein, the reality is likely to be more complex. The enhanced stabilization of the intermediate (F_{hump}) suggests that hydrogen–deuterium exchange has occurred in the region of the A and B β -strands, thereby strengthening the important hydrogen bonds in this region. Indeed, this view is in agreement with previous NMR studies on I27, which found that fast exchange of hydrogen occurs in the A β -strand of the protein, which is likely to have higher flexibility, while the remaining hydrogen atoms were stable for at least 1 day.^[63] Further studies using NMR spectroscopy and SMD simulations should shed light on the detailed timescales and locations of hydrogen deuterium exchange within the protein I27.

2.3. Force-Clamp Unfolding of I27 in D₂

Extending a polyprotein at constant force gives a very different perspective on the unfolding events (Figure 1C). With this approach, the length of an extending polyprotein is measured while the pulling force is actively kept constant by negative feedback control.^[37] The force-clamp technique combined with polyprotein engineering has become a powerful approach to studying proteins. Using this technique, we have investigated the force-dependency of protein folding,^[46,47] unfolding^[37,39,64,65] and of chemical reactions.^[43,44,49] From the force-

dependence, we extract features of the transition state of these reactions that reveal details of the underlying molecular mechanisms. We have determined the properties of the mechanical unfolding transition state of I27₈ by measuring the force dependency of the unfolding rate of single I27₈ polyproteins.^[37] When a protein is subjected to an external force its unfolding rate, k_u , is well described by an Arrhenius term of the form $k_u(F) = k_u^0 \exp(F\Delta x_u/k_B T)$ where k_u^0 is the unfolding rate in the absence of external forces, F is the applied force and Δx_u is the distance from the native state to the transition state along the pulling direction.^[39,45] By measuring how the unfolding rate changes with an applied force, we can obtain estimates for the values of both k_u^0 and Δx_u . Given that $k_u^0 = A \exp(-\Delta G_u/k_B T)$ and assuming a pre-factor, $A \sim 10^{13} \text{ s}^{-1}$,^[39] we can estimate the size of the activation energy barrier of unfolding ΔG_u . The distance to the transition state, Δx_u , determines the sensitivity of the unfolding rate to the pulling force and measures the elongation of the protein at the transition state of unfolding. Given that both k_u^0 and Δx_u reflect properties of the transition state of unfolding, we expect these variables to be strongly influenced by the solvent hydrogen bonding properties of the solvent environment.

Under force-clamp conditions, stretching a polyprotein results in a well-defined series of step increases in length, marking the unfolding and extension of the individual modules in the chain.^[37] The size of the observed steps corresponds to the number of amino acids released by each unfolding event.^[66] Stretching a single I27₈ polyprotein in H₂O at a constant force of 200 pN results in a series of step increases in length of 24 nm (Figure 3A). The time course of these events is a direct

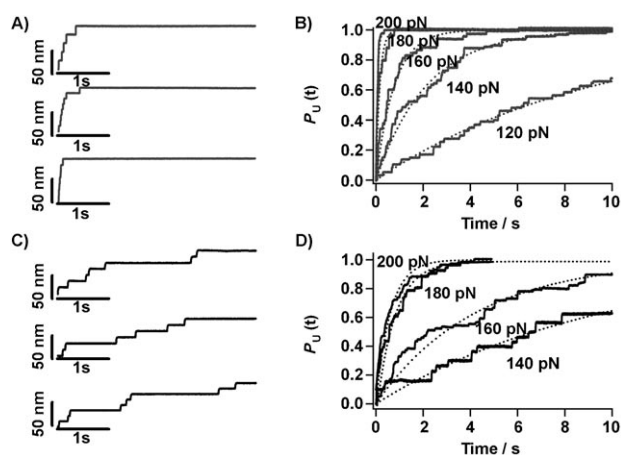


Figure 3. A) Force-clamp unfolding of I27 in H₂O at 200 pN. Three different unfolding traces are shown with the characteristic staircase of unfolding events, with each step of 24 nm corresponding to the unfolding of one module of the polyprotein. The average time course of unfolding is obtained by summation and normalization of $n > 20$ recordings. B) Multiple trace averages of unfolding events measured using force-clamp spectroscopy for I27 in H₂O for constant force measurements at 200 pN, 180 pN, 160 pN, 140 pN and 120 pN. C) Force-clamp unfolding of I27 in D₂O at 200 pN. Again, three different unfolding traces are shown with the characteristic staircase of unfolding events with steps lengths of 24 nm. D) Multiple-trace averages ($n > 20$ in each trace) of unfolding events measured using force-clamp spectroscopy for I27 in D₂O for constant force measurements at 200 pN, 180 pN, 160 pN and 140 pN

measure of the unfolding rate at 200 pN. We measure the unfolding rate by fitting a single exponential to an average of 20 traces similar to the ones shown in Figure 3A. We define the unfolding rate as $k_u(F) = 1/\tau(F)$, where $\tau(F)$ is the time constant of the exponential fits to the averaged unfolding traces, shown in Figure 3B. Furthermore, we obtain an estimate of the standard error of $k_u(F)$, using the bootstrapping technique.^[49,67] We repeated these measurements over the force range between 120 pN and 220 pN and obtained the force-dependency of the unfolding rate in H₂O (Figure 3B). In order to probe the role of solvent hydrogen bonding in the unfolding transition state of I27₈, we studied the effect of substituting H₂O with D₂O on the force dependency of the unfolding rate. Stretching a single I27₈ polyprotein in D₂O at a constant force of 200 pN resulted in a series of step increases of 24 nm (Figure 3C). Upon repeating these measurements over the force range 140 pN to 200 pN, we obtained the force-dependency of the unfolding rate in D₂O (Figure 3D). From the averaged unfolding traces and their corresponding exponential fits obtained at different forces, the force-dependency of the unfolding rate for I27₈ in D₂O was obtained (Figure 4). We fitted the Arrhenius rate

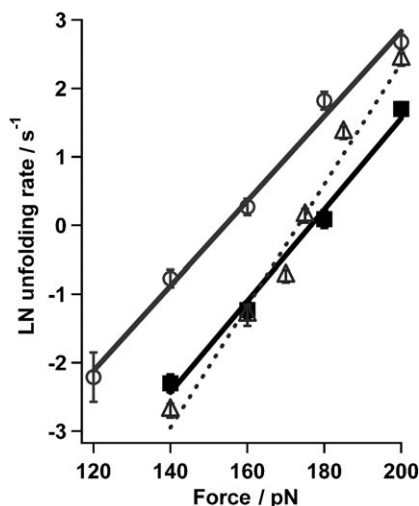


Figure 4. Force-clamp protein unfolding: semi-logarithmic plot of the rate of unfolding of I27 as a function of pulling force in H₂O (○), D₂O (■) and a 20% v/v glycerol solution (△). The lines are a fit of the Arrhenius term,^[45] $\Delta G_u = 23.11 \pm 0.05 \text{ kcal mol}^{-1}$ and $\Delta x_u = 2.5 \text{ \AA} \pm 0.01$ for H₂O, $\Delta G_u = 24.07 \pm 0.03 \text{ kcal mol}^{-1}$ and $\Delta x_u = 2.6 \pm 0.04 \text{ \AA}$ for D₂O, $\Delta G_u = 26.16 \pm 0.05 \text{ kcal mol}^{-1}$ and $\Delta x_u = 4.0 \text{ \AA} \pm 0.01$ for 20% v/v glycerol.

equation to the unfolding rate as a function of pulling force, and obtained $\Delta G_u = 23.11 \pm 0.05 \text{ kcal mol}^{-1}$ and $\Delta x_u = 2.5 \pm 0.1 \text{ \AA}$ for H₂O (Figure 4, ○) and $24.07 \pm 0.03 \text{ kcal mol}^{-1}$ and $\Delta x_u = 2.6 \pm 0.4 \text{ \AA}$ for D₂O (Figure 4, ■).^[39] These experiments showed that replacing H₂O by D₂O has a large effect on the force dependency of unfolding. Interestingly, while the introduction of D₂O increased the value of ΔG_u by ~5%, the Δx_u changed very little. Conversely, previous experiments on the force dependency of unfolding I27 in aqueous glycerol solutions determined that an increase in ΔG_u of ~13% coincided with a significant increase of 1.5 Å in Δx_u (Figure 4, △).^[39] Therefore, while the protein I27 is stabilized in both D₂O and

an aqueous glycerol solution, the distance to the mechanical unfolding transition state is only modified in the presence of a larger solvent molecule, glycerol, and not in the presence of a similarly sized molecule D₂O. It is worth noting that the solution viscosity increases for D₂O ($\eta = 1.14 \text{ cP}$) and 20% glycerol ($\eta = 1.94 \text{ cP}$) solutions as compared with H₂O ($\eta = 0.91 \text{ cP}$). Scaling the unfolding rates $k_u(F)$ in Figure 4 with the relative solution viscosity ($\eta/\eta_{\text{H}_2\text{O}}$) results in an increase in ΔG_u of ~4% for D₂O relative to H₂O and an increase in ΔG_u of ~12% for aqueous glycerol relative to H₂O. Therefore, the solution viscosity does not solely account for the measured changes in $k_u(F)$, and consequently ΔG_u . Perhaps more significantly, scaling $k_u(F)$ with the solution viscosity has no effect on the measured value of Δx_u , since the slope of Figure 4 remains unchanged.

2.4. Molecular Interpretation of Δx in Protein Unfolding

SMD can complement our AFM observations by providing a detailed atomic picture of stretching and unfolding individual proteins.^[54,56] The simulations involve the application of an external force to molecules in a molecular dynamics simulation. The SMD simulations are carried out by fixing one terminus of the protein and applying external forces to the other terminus (see the Experimental Methods). Earlier SMD simulations of forced unfolding of the I27 protein suggested that resistance to mechanical unfolding originates from a localized patch of hydrogen bonds between the A' and G β-strands of the protein (Figure 5A).^[54,56] The A' and G strands must slide past one another for unfolding to occur. Since the hydrogen bonds are perpendicular to the axis of extension, they must rupture simultaneously to allow relative movement of the two termini. Thus, these bonds were singled out to be the origin of the main barrier to complete unfolding.^[56] This view was experi-

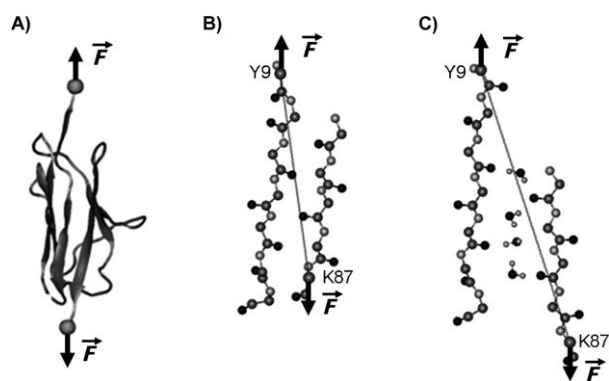


Figure 5. A) Cartoon of the I27 protein highlighting the direction of the pulling forces (arrows). B) Snapshot of the β-strands A' and G of the I27 protein showing the protein backbone only for simplicity. C) Snapshot of the β-strands A' and G of the I27 protein showing 4 D₂O molecules bridging the protein backbone. Steered molecular dynamics simulations measure the elongation of β-strands A' and G for unfolding the I27 protein in D₂O. The pulling coordinate for the separating β-strands is defined as the distance between the first amino acid of strand A' (Y9) and the last amino acid of strand G (K87). The elongation of the x(Y9)–x(K87) distance up to the transition state is defined as the distance $\Delta x_{A'-G}$. The crossing of the transition state is marked by an abrupt rapid increase in x(Y9)–x(K87) that leads to complete unravelling of the protein.

mentally validated by force spectroscopy experiments on I27 with mutations in the A' and G β -strands of the protein.^[53,67] The SMD simulations also showed that water molecules participated in the rupture of the backbone H bonds during the forced extension of the protein.^[56] Although the transition state structure could not be determined from such simulations, the integral role played by the water molecules was highly suggestive of their part in forming the unfolding transition state structure. We recently tested this view by using solvent substitution. In these experiments, water was systematically replaced by the larger molecule glycerol (2.5 Å versus 5.6 Å, respectively).^[39] At each glycerol concentration, the force dependency of the unfolding of I27₈ was measured, yielding values of Δx_u that grew rapidly with the glycerol concentration, reaching a maximum value of $\Delta x_u = 4.4 \pm 0.04$ Å, suggesting that the value of Δx_u follows the size of the solvent molecule. We interpreted these results as an indication that at the transition state, solvent molecules bridge the key A' and G β -strands of the I27 protein.^[39] SMD simulations of forced unfolding of the I27 protein in water and an aqueous glycerol solution directly showed that solvent molecules were bridging the A' and G β -strands of the I27 protein during the main unfolding barrier.^[39] To further validate this view and gain insight into the role of solvent hydrogen bonds in protein unfolding, we repeated these SMD simulations of force unfolding of the I27 protein in D₂O. The simulations were completed using the methods described in the Experimental Section and in detail in previous work.^[39,54,56]

Our SMD simulations of forced unfolding of the I27 protein in D₂O showed that resistance to unfolding still originates from the same set of hydrogen bonds between the A' and G β -strands (Figure 5A). In the constant-velocity simulations, the breaking of the hydrogen bonds between the A' and G β -strands is the mechanical barrier that creates the highest force peak in the force extension curve. Significantly, the force peak during unfolding in D₂O is higher than that in H₂O. The average force peak in D₂O, from three separate SMD simulations, is 2800 pN. In the case of H₂O the average force peak is 1850 pN, consistent with previous SMD simulations.^[56] In constant-force SMD simulations, I27 shows more mechanical strength in D₂O than in H₂O. In H₂O under an external force of 800 pN, I27 readily unfolds after 720 ps. Conversely, in the case of I27 in D₂O, under an external force of 800 pN, the protein does not unfold within the 3 ns timescale of the simulation. The protein only unfolds after 2200 ps when the force is increased to 1200 pN. These simulations showed that the rupture of A' and G β -strands can be facilitated by the breaking of interstrand hydrogen bonds by D₂O molecules. These molecules form bridges between the two separating strands (Figure 5). One way to interpret these results is that the transition state structure is formed by D₂O molecules bridging the gap between separating β -strands. In Figure 5B, we define the pulling coordinate for the A' and G β -strands as the distance between the first amino acid of strand A' (Y9) and the last amino acid of strand G (K87). This distance, $x(Y9)-x(K87)$, increases as the two β -strands separate under a constant force filling the gap with D₂O molecules until the transition state is reached (Fig-

ure 5C). The elongation of the $x(Y9)-x(K87)$ distance up to the transition state is defined as the distance to the transition state $\Delta x_{A'-G}$. Interestingly, $\Delta x_{A'-G}$ remains unchanged in D₂O as compared with H₂O, consistent with our force-clamp experiments and the hypothesis of a solvent bridging mechanism in the mechanical unfolding transition state of this protein. Movement of the transition state away from the folded state with increasingly protective conditions is known from transition state theory as the Hammond effect.^[69] While the Hammond postulate is an appealing description of transition state movement in protein folding, it offers no molecular insight into the mechanisms by which the protein reaches its transition state. Furthermore, the result that D₂O stabilizes the native state of the I27 protein without changing the transition state position suggests that the Hammond postulate is not sufficient. The motivation of our experiments was to go beyond a simple description and propose a molecular model for the solvent-induced changes in the mechanical unfolding transition state of a protein. Our results suggest that D₂O plays an integral role in the unfolding transition state of this protein.

2.5. Probing Protein Collapse Using Force-Ramp Experiments

To examine the role of solvent hydrogen bonds and hydrogen bond strength on the driving forces in protein collapse, we used a force-ramp protocol to measure the collapse trajectories of individual I27₈ proteins in H₂O and D₂O. The force-ramp protocol linearly decreases the force applied to a protein with time and allows for the observation of the full force-length relationship of an extended protein, rather than only discrete force values.^[42] From the force-length behaviour of many individual proteins, we reveal details of the underlying molecular mechanisms and driving forces in protein collapse. Figure 6

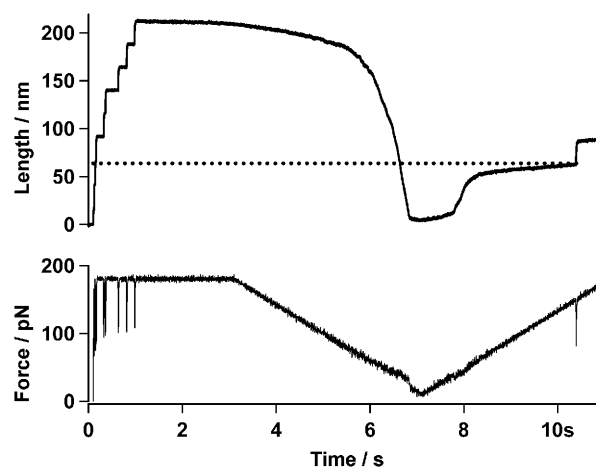


Figure 6. We use a force ramp protocol to examine the nature of the forces driving protein collapse. I27₈ in D₂O is unfolded at a high force of 180 pN. Subsequently, the force is linearly decreased from 180 pN down to 10 pN in 4 sec, and back up to 180 pN to probe refolding. In the example shown while the force is being relaxed, the protein collapses very readily. Protein folding was indicated by a reduction in length of 24 nm upon restoring the force to 180 pN.

shows an example of a collapse trajectory obtained for I27₈ in D₂O. The I27₈ polyprotein was first unfolded at a high force of 180 pN. Subsequently, the force was ramped from 180 pN down to 10 pN in 4 seconds and protein collapse was observed. Finally the force was ramped back up to 180 pN to determine whether the protein successfully folded during the experiment. In the example shown while the force was being relaxed, the protein collapsed very readily, reaching a length close to that of the folded protein. To confirm that the protein had indeed folded, the force was ramped back up to 180 pN. Successfully folded proteins were detected by a decrease in length by multiples of ~24 nm following restoration of the force to 180 pN (Figure 6). In order to compare all collapse trajectories, we normalized their length by the value measured in the initial extended conformation at 180 pN. The normalized length is shown in Figure 7 as a function of the force during the ramp down to 10 pN for I27₈ in H₂O (upper panel) and in D₂O (lower panel). In both cases we observe a surprising degree of heterogeneity in the responses in agreement with earlier work on the polyprotein ubiquitin.^[42] Proteins that failed to fold during the ramp (grey traces, $n=85$ for H₂O and $n=64$

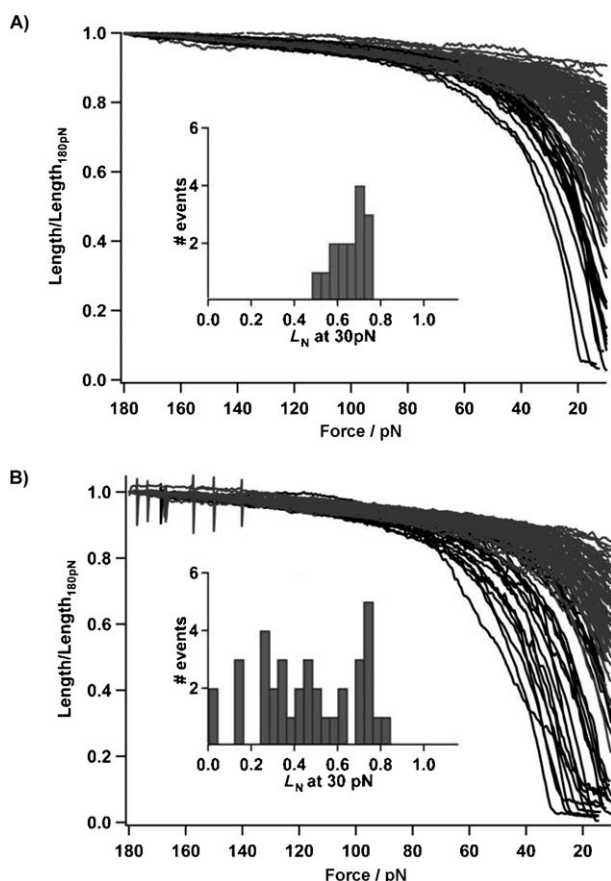


Figure 7. To compare all recordings from the force-ramp experiments, the protein length during the ramp is normalized by its value for the extended conformation at 180 pN. This normalized length, $\text{Length}/\text{Length}_{180\text{pN}}$, is shown as a function of force during the ramp down to 10 pN (folds in black, failures in grey) for H₂O (top) and D₂O (bottom). Inset: Histograms of $\text{Length}/\text{Length}_{180\text{pN}}$ at 30 pN for H₂O (top) and D₂O (bottom). At this force, there is a larger distribution of proteins which have significantly contracted in length in D₂O as compared with H₂O.

for D₂O) show large variations in their collapse. By contrast, proteins that folded (black traces, $n=15$ for H₂O and $n=36$ for D₂O) collapse much further resulting in smaller values of L_N . Strikingly, the number of successfully folding I27 proteins increases significantly in the presence of D₂O. This is apparent from the histogram of L_N measured at 30 pN in H₂O (upper inset) and in D₂O (lower inset) for proteins that folded successfully. In the case of H₂O, most of the proteins remain very elongated even at low forces of 30 pN. Strikingly, in the case of I27₈ in D₂O, we observe that this distribution shifts to lower L_N values. Therefore, the driving forces which allow the protein to collapse and subsequently fold in D₂O are already present at these forces of 30 pN. It is interesting to consider which molecular interactions would dominate at these length scales and could enhance protein collapse.

Single-molecule force spectroscopy experiments demonstrate that protein folding is a highly heterogeneous process where the collapsing polypeptide visits broad ensembles of conformations of increasingly reduced dimensionality. Upon substitution of H₂O with the stronger hydrogen bonding solvent D₂O, an enhancement in the collapse of the extended polyprotein is observed (Figure 7). These experimental results and the observation of a heterogeneous ensemble of collapse trajectories are in excellent agreement with the statistical theories of protein folding developed over a decade ago,^[70–73] which have remained inaccessible in bulk experiments. The new challenge is to develop and refine theoretical descriptions of protein collapse. Significantly, these new models can now make use of information obtained from single-molecule experiments to characterize the strength and variability of protein collapse.

2.6. Identifying the Nature of the Underlying Interactions in Protein Folding

To probe the role of solvent hydrogen bonds and hydrogen bond strength on the driving forces in protein folding, we used a force-quench protocol to measure the folding trajectories of individual I27₈ proteins in H₂O and D₂O. Force-quench experiments on polyproteins have permitted the capture of individual unfolding and folding trajectories of a single protein under the effect of a constant stretching force.^[41,47] This experimental approach allows the dissection of individual folding trajectories and provides access to the physical mechanisms that govern each stage in the folding trajectory of a protein. In the force-quench protocol, the protein is first stretched at a high force to prompt unfolding (Figure 8A, B). Subsequently the force is quenched to trigger collapse and the protein's journey towards the ensemble of native conformations is monitored as a function of length over time. In order to confirm that the protein has indeed folded, the force is again increased to unfold the same molecule.

In the two examples shown in Figures 8A and B we observe a staircase of unfolding events consisting of step increases in length of 24 nm corresponding to the unfolding of each module in the polyprotein chain. After 3 seconds, the pulling force was quenched down to 10 pN (Figure 8A) and 40 pN

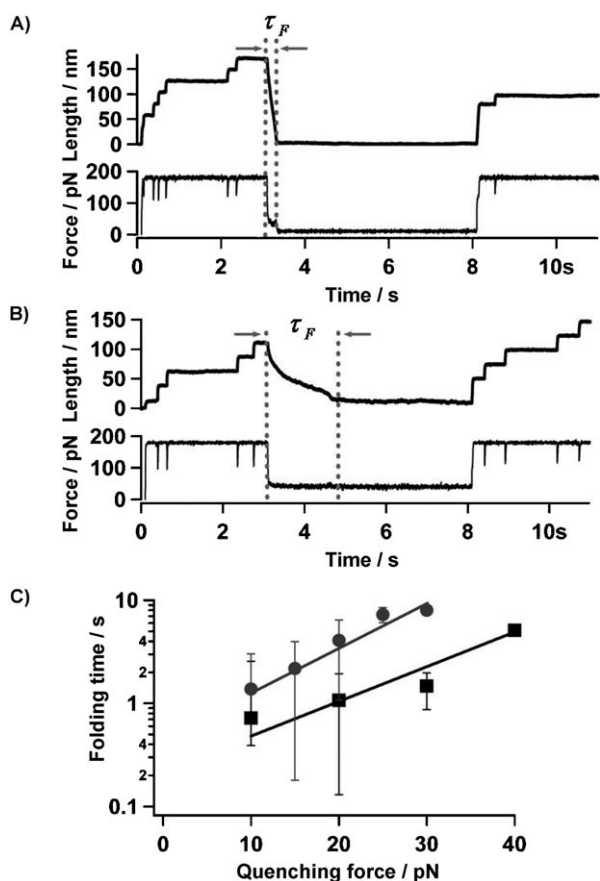


Figure 8. Force quench experiments reveal the folding trajectory of a single polyprotein in D₂O. A) The folding pathway of I27₈ is directly measured by force-clamp spectroscopy. The end-to-end length of a protein is shown as a function of time. The length of the protein (nm) evolves in time as it first extends by unfolding at a constant stretching force of ~180 pN. Upon quenching the force to ~10 pN, the protein collapses to its folded length. After the protein has collapsed, it acquires the final native contacts that define the native fold. To confirm that the protein had indeed folded, at 8 seconds we stretched back again at a force of 180 pN, registering a new staircase of unfolding events (5). B) In the second example 4 modules in the polyprotein unfold. Upon quenching the force to ~40 pN, the protein collapses to its folded length. After stretching the protein again at ~180 pN, two of the four modules unfold again, bringing the polyprotein to its original unfolded length. Subsequently a further two modules in the polyprotein unfold. The corresponding applied force is also shown as a function of time. C) The mean time of the collapse trajectories is very strongly force dependent. Logarithmic plot of the folding time, τ , as a function of the quenching force, for the polyprotein I27₈ in H₂O^[46] (●) and D₂O (■) are shown. Data are fitted to an exponential relationship, yielding $\tau(F) = 0.52 \exp(F \times 0.1)$ for I27₈ in H₂O (—) and $\tau(F) = 0.22 \exp(F \times 0.08)$ for I27₈ in D₂O (—). The folding times in the absence of force give rise to folding rates of $1/\tau_{OF} = 1.92 \text{ s}^{-1}$ for I27₈ in H₂O and 4.55 s^{-1} for I27₈ in D₂O, while the value of Δx_F changes from 4.1 Å in H₂O to 3.2 Å in D₂O.

(Figure 8B) and the protein collapsed and subsequently folded. It should be noted that a broad range of collapse times to the folded length are observed even at a constant force, due to the rough energy landscape underlying the folding process.^[41,47] The protein collapses to different extents depending on the quenched force.^[47] On average, the higher the quenching force, F_Q the longer the folding time, τ_F , defined as the time at which the trajectories reach the base line (folded length), as illustrated in the Figures 8A and B. Figure 8C shows

the folding time at a range of force from 15 pN to 40 pN and demonstrates that the mean time of the collapse trajectories is very strongly force dependent. A logarithmic plot of τ_F as a function of the F_Q for the polyprotein I27₈ in H₂O^[46] (●) and D₂O (■) are shown. Data were fitted to an exponential relationship, yielding $\tau_F = 0.52 \exp(F \times 0.1)$ for I27₈ in H₂O (—) and $\tau_F = 0.22 \exp(F \times 0.08)$ for I27₈ in D₂O (—). The distance to the folding transition state Δx_F changes from 4.1 Å in H₂O to 3.2 Å in D₂O. Interestingly, the value of Δx for folding is much larger than that measured for unfolding and may reflect the role of distant residues and longer-range forces acting in the collapse trajectories.^[47] The folding times in the absence of force give rise to folding rates of $1/\tau_{OF} = 1.92 \text{ s}^{-1}$ for I27₈ in H₂O and 4.55 s^{-1} for I27₈ in D₂O. Upon increasing the hydrogen bond strength of the solvent environment by ~0.2 kcal mol⁻¹, an increase in the folding rate of I27 is observed. If we consider the driving force in protein folding to be hydrophobic collapse, then these single-molecule experiments suggest that the hydrophobic effect is enhanced in D₂O as compared to H₂O.^[42,74] Significantly, these results provide the first single-molecule-level measurement of the influence of D₂O on the hydrophobic effect during protein folding.

2.7. The Force Dependency of Chemical Reactions

In the previous sections we have shown how force-clamp spectroscopy can be used to probe the role of solvent hydrogen bonds in protein unfolding, collapse and folding. However, protein unfolding and refolding are complex processes, potentially involving thousands of atoms. Here we show that force-clamp spectroscopy can be used to probe a simple system, composed of only a few atoms, to carefully monitor the transition state structure of a chemical reaction. To identify the role of solvent hydrogen bond strength on the force dependency of a chemical reaction, we completed a series of force-clamp experiments to examine the reduction of individual disulfide bonds in a protein molecule in both H₂O and D₂O. Using this technique we can identify not only a transition state structure on a sub-Ångstrom scale, but also identify how mechanical forces can influence chemical kinetics.^[43,44,49] Using a protein with an engineered disulfide bond, we measured the rate of disulfide bond reduction in the presence of different reducing agents in D₂O solution. Specifically, we engineered a polyprotein with repeats of the I27 module which were mutated to incorporate two cysteine residues (G32C, A75C).^[44] The two cysteine residues spontaneously form a stable disulfide bond that is buried in the β -sandwich fold of the I27 protein. We call this polyprotein (I27_{S-S})₈. The disulfide bond mechanically separates the I27 protein into two parts. The grey region of unsequestered amino acids readily unfolds and extends under a stretching force (Figure 9A). The black region marks 43 amino acids which are trapped behind the disulfide bond and can only be extended if the disulfide bond is reduced by a nucleophile.^[43,44,49,66] We used force-clamp AFM to extend single (I27_{S-S})₈ polyproteins. The constant force caused individual I27 proteins in the chain to unfold, resulting in stepwise increases in length of the molecule following each unfolding event.

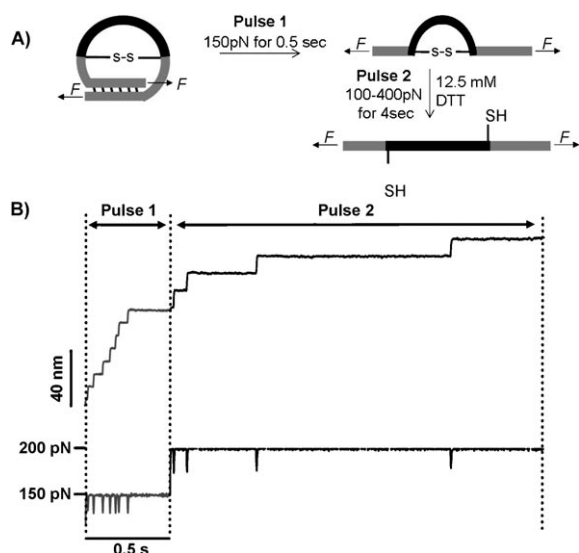


Figure 9. Reduction of protein disulfide bonds in the presence of a disulfide reducing agent observed by the single-molecule force-clamp technique. A) Diagram showing modified I27, I27_{G32C-A75C}, with an engineered disulfide bond (Cys32–Cys75), being pulled by an atomic force microscope cantilever in two steps: Pulse 1 includes the mechanical stretching of the protein and exposing the sequestered disulfide bond. Pulse 2 is the reduction of the disulfide bond in the presence of a reducing agent. B) Extension profile of the protein, (I27_{G32C-A75C})₈, in 12.5 mM DTT (in D₂O PBS buffer, pH 7.4). Unfolding steps (~11 nm) in pulse 1 are due to the stretching of individual protein modules under force (150 pN) whereas the steps in pulse 2 (13.5 nm at 200 pN) correspond to the reduction of individual disulfide bonds and stretching the remaining polypeptide between the cysteines.

However, this unfolding is limited to the “unsequestered” residues by the presence of the intact disulfide bond, which cannot be ruptured by force alone. After unfolding, the stretching force is applied directly to the disulfide bond, now exposed to solvent. If a reducing agent is present in the bathing solution, the bond can be chemically reduced. In order to study the kinetics of disulfide bond reduction as a function of the pulling force, we utilized a double-pulse protocol in force-clamp. Figure 9B demonstrates the use of the double-pulse protocol using dithiothreitol (DTT) as the reducing agent in D₂O. The first pulse to 150 pN results in a rapid series of steps of ~11 nm marking the unfolding and extension of the unsequestered residues. After exposing the disulfide bonds to the solution by unfolding, we track the rate of reduction of the exposed disulfides with a second pulse at a particular force, in the presence of the reducing agents. In the absence of DTT, no steps are observed during the test pulse. However, in the presence of DTT (~12.5 mM) a series of ~13.5 nm steps follow the unfolding staircase. Each 13.5 nm step is due to the extension of the trapped residues, unambiguously marking the reduction of each module in the (I27_{S-S})₈ polyprotein. We measure the rate of disulfide bond reduction at a given force by fitting a single exponential to an ensemble average of 10–30 traces. We calculate the rate constant of reduction as $r = 1/\tau_r$ where τ_r is the time constant measured from the exponential fits. Figure 10A shows a plot of the rate of reduction, r , as a function of force for experiments done in the presence of DTT in a D₂O solution (■). Over a range of 100 pN to 400 pN of applied force

the rate of disulfide bond reduction was accelerated, demonstrating that mechanical force can indeed catalyze this chemical reaction. The observed force dependence of the rate of disulfide bond reduction by DTT was found to be much less sensitive than the rate of I27 unfolding.^[44] Through a simple Arrhenius fit to these data, we found that this force dependent increase in the reduction rate can be explained by an elongation of the disulfide bond by $\Delta x_r = 0.37 \pm 0.04$ Å, at the transition state of the S_N2 chemical reaction. Remarkably, the measured distance to the transition state of this S_N2 type chemical reaction was in close agreement with disulfide bond lengthening at the transition state of thiol-disulfide exchange as found by DFT calculations.^[75] This result indicates that the force-dependence of the observed reaction kinetics is governed by the detected sub-Ångstrom length changes between the two sulfur atoms at the reaction transition state. For the nucleophile tris(2-carboxyethyl)phosphine (TCEP), a larger bond elongation of $\Delta x = 0.41 \pm 0.04$ Å at the transition state of the reaction was measured (Figure 10B), in agreement with quantum mechanical calculations of the transition state structures.^[43] To probe the effect of solvent hydrogen bonding on the rate of disulfide bond reduction we compared these experiments with those using the reducing agents DTT and TCEP in H₂O and a 30% v/v glycerol solution.^[43] Figures 10A and B show the force dependency for each reducing agent in the three solvent environments. In the case of DTT, Δx_r was measured to increase slightly from 0.34 ± 0.05 Å in H₂O to 0.37 ± 0.04 Å in D₂O while for TCEP, Δx_r was measured to decrease from 0.46 ± 0.03 Å in H₂O to 0.41 ± 0.04 Å in D₂O. Therefore, perhaps surprisingly, the measured values of Δx_r in D₂O do not differ significantly from that measured in H₂O. This is in contrast with the results from

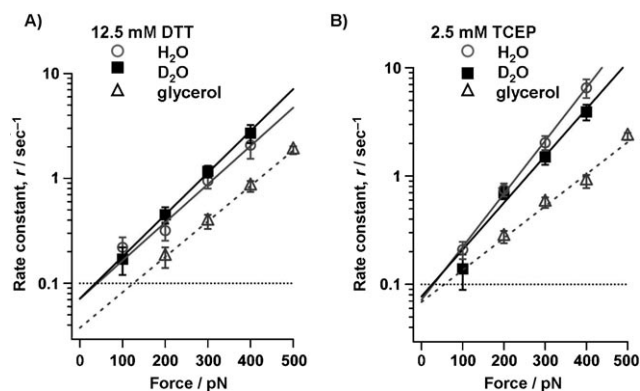


Figure 10. Comparison of force-dependent rate constants for disulfide bond reduction in H₂O, D₂O and a 30% v/v glycerol solution. A) The rate constant for the disulfide-bond reduction by DTT remains relatively unchanged when changing the solvent from H₂O (○) to D₂O (■). Fitting with the Arrhenius model (thick line) gives a distance to the transition state, $\Delta x_r = 0.34 \pm 0.05$ Å in H₂O and 0.37 ± 0.04 Å in D₂O and an activation energy, $E_A = 54.3 \pm 0.8$ kJ mol⁻¹ in H₂O and 54.3 ± 0.7 kJ mol⁻¹ in D₂O. B) In the case of disulfide-bond reduction by TCEP the rate constant also remain relatively unchanged and $\Delta x_r = 0.46 \pm 0.03$ Å in H₂O and 0.41 ± 0.04 Å in D₂O and an activation energy, $E_A = 58.3 \pm 0.5$ kJ mol⁻¹ in H₂O and 58.1 ± 0.6 kJ mol⁻¹ in D₂O. These results suggest that the transition state structure remains unchanged when the solvent environment is changed from H₂O to D₂O. By contrast, the rate constants for the disulfide-bond reduction by DTT change significantly when changing the solvent to 30% v/v glycerol (△).

glycerol experiments were the force dependency of disulfide bond reduction was very sensitive to glycerol content.^[43]

It has previously been suggested that the reduction of disulfide bonds proceeds via a biomolecular nucleophilic substitution mechanism^[75] in which transport of a proton along a water wire is responsible for the simultaneous deprotonation of the arriving sulfur and protonation of the departing sulfur.^[43] In this view, coupled to the external proton transfer is the motion of the sulfur atom, representing the actual S_N2 type of displacement which leads to reduction of the disulfide bond. Importantly, proton transfer in water is strongly controlled by the hydrogen bond network.^[76–79] The observation that Δx_r is unaffected by the strength of hydrogen bonds in the water suggests that proton transfer is not the rate determining step in the reduction of a disulfide bond by DTT or TCEP. Instead, it is possible that the collision mechanism between the disulfide bond and the reducing agent determines the molecular details of Δx_r . Indeed, the experimental measurements of the activation energy E_A for reduction by DTT and TCEP in H_2O and D_2O appear to support this hypothesis (Figure 10). In the case of the reducing agent DTT, E_A was unchanged when H_2O was changed to D_2O while for TCEP, Δx_r was measured to decrease very slightly from $58.3 \pm 0.5 \text{ kJ mol}^{-1}$ in H_2O to $58.1 \pm 0.6 \text{ kJ mol}^{-1}$ in D_2O . Therefore, the measured values of E_A in D_2O do not differ significantly from that measured in H_2O . It is expected that an isotopic substitution will greatly modify the reaction rate when the isotopic replacement is in a chemical bond that is broken or formed in the rate limiting step of a reaction.^[80] In this case, the rate change is termed a primary isotope effect. Alternatively, when the substitution is not involved in the bond that is breaking or forming, a smaller rate change would be expected, termed a secondary isotope effect. Indeed, the magnitude of the kinetic isotope effect is often used to elucidate the reaction mechanism and if other effects are partially rate-determining, the effect of isotopic substitution may be masked.^[81] The results presented here suggest that the bond breakage and reformation of the substrate and the reducing agent is the main determinant in the force dependency of disulfide bond reduction. Interestingly, this hypothesis could be pursued by completing force-clamp spectroscopy experiments on the protein (I27_{S5})₈ in a solution containing an isotopically substituted reducing agent. These experiments may hold promise for developing a quantitative view of a disulfide bond reduction and the role of hydrogen bonding in chemical reactions, at a resolution currently unattainable by any other means. The present experiments illustrate that the sub-Ångstrom resolution of the transition state dynamics of a chemical reaction obtained using force-clamp techniques makes a novel contribution to our understanding of protein based chemical reactions.

3. Conclusions

Using a combination of force protocols we have demonstrated that protein unfolding, protein collapse, protein folding and chemical reactions are affected in very different ways by the substitution of H_2O with D_2O . Although the increase in hydro-

gen bond strength of the solvent environment upon substitution is small ($\sim 0.2 \text{ kcal mol}^{-1}$), single molecule force spectroscopy has identified significant changes in these protein based reactions. We have found that D_2O molecules play an integral role during protein unfolding, where they form a bridge in the unfolding transition state of the protein I27. A striking result from this work is that D_2O is a worse solvent than H_2O for the I27 protein and hydrophobic interactions are enhanced. This is apparent as an increase in ΔG_u (Figure 4) and a marked enhancement in the hydrophobic collapse trajectories (Figure 7) and folding trajectories (Figure 8) of the protein. Significantly, this result is in direct contrast with experiments^[17–20] and theoretical studies^[21–23] on simple hydrocarbons and noble gases which show that D_2O is a better solvent than H_2O . Interestingly, while an increase in hydrogen bond strength of the solvent environment has a significant effect on protein unfolding and folding we find that a chemical reaction is unaffected. Indeed, we measure no detectable change in the force dependent rate of reduction of a disulfide bond engineered within a single I27 protein upon substituting H_2O with D_2O . By contrast, previous work has shown that the force dependent rate of reduction of a disulfide bond is greatly affected upon substitution of H_2O by the larger solvent molecule glycerol. Our new results suggest that the transition state for this chemical reaction may be sensitive to the size of molecules in the solvent environment but not to their hydrogen bond strength.

These preliminary experiments illustrate the potential of single molecule force spectroscopy in determining the role of hydrogen bonds in protein based reactions. While the present work has focused on the hydrogen bond strength of the solvent environment, further studies will examine the importance of hydrogen bonds within the protein. By substituting hydrogen with deuterium in the protein we will measure the force dependency of a range of protein reactions and determine how the dynamics is linked to the strength of hydrogen bonds in the system. Using a single-molecule approach it becomes possible to experimentally investigate the molecular mechanisms involved in these processes. The dynamics of protein folding and chemical reactions is intrinsically linked to the structure of the transition state. By designing and implementing force protocols the force dependency of a reaction can easily be obtained, providing detailed information on the transition state of interest. Through continued examination and the development and refinement of theoretical models further progress could be made in understanding the molecular mechanism in protein folding and chemical reactions.

Experimental Section

Protein Engineering and Purification: We constructed an eight domain N-C linked polyprotein of I27, the 27th immunoglobulin-like domain of cardiac titin, through successive cloning in modified pT7Blue vectors and then expressed the gene using vector pQE30 in *Escherichia coli* strain BLR(DE3). The protein was stored at 4°C in 50 mM sodium phosphate/150 mM sodium chloride buffer (pH 7.2). The details of the polyprotein engineering and purification have been reported previously.^[50]

Solvent Environment: Samples of deuterium oxide were obtained from Sigma–Aldrich and used without additional purification. Experiments were carried out in H₂O or D₂O PBS buffer at pH 7.2. Deuterium oxide solutions were carefully prepared to ensure the same salt concentration and pH as that of PBS buffer.

Single-Molecule Force Spectroscopy: We used a custom-built atomic force microscope equipped with a PicoCube P363.3-CD piezoelectric translator (Physik Instrumente, Karlsruhe, Germany) controlled by an analog PID feedback system that has been described previously. Silicon-nitride cantilevers (Veeco, Santa Barbara, CA) were calibrated for their spring constant using the equipartition theorem. The average spring constant was ~ 15 pN nm⁻¹ for force-clamp experiments and ~ 60 pN nm⁻¹ for force-extension experiments. All data was obtained and analyzed using custom software written for use in Igor 5.0 (Wavemetrics, Oswego, OR). There was approximately 0.5 nm of peak-to-peak noise and a feedback response time of ~ 5 ms in all experiments. To estimate the error on our experimentally obtained rate constant, we carried out the non-parametric bootstrap method.^[49,67] In the AFM experiments, an O-ring was used to minimize the rate of evaporation of the solvent buffer. The O-ring fits into the fluid cell and allows a seal to be formed for the protein in solution between the fluid cell and the coverslip.

Steered Molecular Dynamics Simulations: The I27 protein was subject to a simulated equilibration, constant velocity SMD, and constant force SMD. The aqueous environment was modelled using explicit water with periodic boundary conditions. D₂O potentials were adopted from the SPC/HW model.^[82] This potential has been compared with experimental data on diffusion coefficient, dipole moment, density and vaporization heat.^[82] We make the assumption that hydrogen and deuterium do not exchange in the time-scale of the simulation.^[63,83] The water box was large enough for equilibration and for the first 50 Å of stretching (length 135 Å, width 68 Å, height 68 Å). The whole protein water system contained ~ 59300 atoms. The D₂O box has the same size as the pure water box. The corresponding molecular structure file (.psf) was generated by psfgen in VMD based on the structure of the I27 protein and water molecules. The total system of protein-water contains 60165 atoms. The velocities used in constant velocity SMD simulations were 10 ms⁻¹, 6 orders of magnitude larger than pulling velocities used in AFM experiments. The I27 protein was also stretched by the clamped forces at 800, 1000, 1200, 1500, 1800 and 2000 pN, separately, in the constant force SMD simulations. The model preparation and data analysis were done with VMD^[84] and MD simulation with NAMD.^[85] During the 1 ns equilibration the protein is reasonably stable and did not deviate from the initial PDB structure 1TIT, with the RMSD below 1.6 Å. That final structure from the equilibration was the starting structure in the constant velocity and constant force SMD.

Acknowledgements

We are grateful to Sergi Garcia-Manyes for careful reading of the manuscript and Pallav Kosuri for assistance in figure preparation. This work was supported by NIH grants to J.M.F. (HL66030 and HL61228).

Keywords: hydrogen bonds • proteins • single-molecule studies • solvent effects • transition states

- [1] G. D. Rose, R. Wolfenden, *Annu. Rev. Biophys. Biomol. Struct.* **1993**, *22*, 381–415.
- [2] J. Israelachvili, *Intermolecular and Surface Forces*, Academic Press, New York, **1991**.
- [3] C. Tanford, *The Hydrophobic Effect: Formation of Micelles and Biological Membranes*, Krieger, New York, **1991**.
- [4] T. S. Moore, T. F. Winmill, *J. Chem. Soc.* **1912**, *101*, 1635–1676.
- [5] L. Pauling, R. B. Corey, *Proc. Natl. Acad. Sci. USA* **1951**, *37*, 251–256.
- [6] L. Pauling, R. B. Corey, *Nature* **1951**, *168*, 550–551.
- [7] L. Pauling, R. B. Corey, *Proc. Natl. Acad. Sci. USA* **1953**, *39*, 253–256.
- [8] G. C. Pimental, A. L. McClellan, *The Hydrogen Bond*, Freeman, San Francisco, **1960**.
- [9] E. N. Baker, R. E. Hubbard, *Prog. Biophys. Mol. Biol.* **1984**, *44*, 97–179.
- [10] A. Fernández, T. R. Sosnick, A. Colubri, *J. Mol. Biol.* **2002**, *321*, 659–675.
- [11] G. A. Jeffrey, W. Saenger, *Hydrogen Bonding in Biological Structures*, Springer, Heidelberg, **1991**.
- [12] S. Y. Sheu, E. W. Schlag, H. L. Selzle, D. Y. Yang, *J. Phys. Chem. A* **2008**, *112*, 797–802.
- [13] A. K. Soper, C. J. Benmore, *Phys. Rev. Lett.* **2008**, *101*, 065502.
- [14] A. K. Soper, *J. Phys. Condens. Matter* **2007**, *19*, 1–18.
- [15] L. Benjamin, G. C. Benson, *J. Phys. Chem.* **1963**, *67*, 858–861.
- [16] S. Scheiner, M. Cuma, *J. Am. Chem. Soc.* **1996**, *118*, 1511–1521.
- [17] G. C. Kresheck, H. Schneide, H. A. Scheraga, *J. Phys. Chem.* **1965**, *69*, 3132–3144.
- [18] M. M. Lopez, G. I. Makhatazde, *Biophys. Chem.* **1998**, *74*, 117–125.
- [19] Y. Marcus, A. Bennaïm, *J. Chem. Phys.* **1985**, *83*, 4744–4759.
- [20] E. Wilhelm, R. Battino, R. J. Wilcock, *Chem. Rev.* **1977**, *77*, 219–262.
- [21] G. Hummer, S. Garde, A. E. Garcia, L. R. Pratt, *Chem. Phys.* **2000**, *258*, 349–370.
- [22] G. Graziano, *J. Chem. Phys.* **2004**, *121*, 1878–1882.
- [23] J. H. Griffith, H. A. Scheraga, *J. Mol. Struct.* **2004**, *682*, 97–113.
- [24] R. H. Maybury, J. J. Katz, *Nature* **1956**, *177*, 629–630.
- [25] M. J. Parker, A. R. Clarke, *Biochemistry* **1997**, *36*, 5786–5794.
- [26] P. A. Baghurst, W. H. Sawyer, L. W. Nichol, *J. Biol. Chem.* **1972**, *247*, 3198–3208.
- [27] G. Chakrabarti, S. Kim, M. L. Gupta, J. S. Barton, R. H. Himes, *Biochemistry* **1999**, *38*, 3067–3072.
- [28] H. Omori, M. Kuroda, H. Naora, H. Takeda, Y. Nio, H. Otani, K. Tamura, *Eur. J. Cell Biol.* **1997**, *74*, 273–280.
- [29] R. Guzzi, L. Sportelli, C. LaRosa, D. Milardi, D. Grasso, *Prog. Biophys. Mol. Biol.* **1996**, *65*, 61.
- [30] B. Kuhlman, D. P. Raleigh, *Protein Sci.* **1998**, *7*, 2405–2412.
- [31] G. I. Makhatazde, G. M. Clore, A. M. Gronenborn, *Nat. Struct. Biol.* **1995**, *2*, 852–855.
- [32] Y. K. Cheng, P. J. Rossky, *Nature* **1998**, *392*, 696–699.
- [33] N. Giovambattista, C. F. Lopez, P. J. Rossky, P. G. Debenedetti, *Proc. Natl. Acad. Sci. USA* **2008**, *105*, 2274–2279.
- [34] B. A. Patel, P. G. Debenedetti, F. H. Stillinger, P. J. Rossky, *J. Chem. Phys.* **2008**, *128*, 175102–175116.
- [35] F. Pizzitutti, M. Marchi, F. Sterpone, P. J. Rossky, *J. Phys. Chem. B* **2007**, *111*, 7584–7590.
- [36] P. Cioni, G. B. Strambini, *Biophys. J.* **2002**, *82*, 3246–3253.
- [37] M. Schlierf, H. Li, J. M. Fernandez, *Proc. Natl. Acad. Sci. USA* **2004**, *101*, 7299–7304.
- [38] Y. Cao, H. Li, *J. Mol. Biol.* **2008**, *375*, 316–324.
- [39] L. Dougan, G. Fang, H. Lu, J. M. Fernandez, *Proc. Natl. Acad. Sci. USA* **2008**, *105*, 3185–3190.
- [40] L. Dougan, J. M. Fernandez, *J. Phys. Chem. A* **2007**, *111*, 12402–12408.
- [41] S. Garcia-Manyes, L. Dougan, C. M. Badilla, J. Brujic, J. M. Fernandez, unpublished results.
- [42] K. Walther, F. Grater, L. Dougan, B. C. L. B. J. Berne, J. M. Fernandez, *Proc. Natl. Acad. Sci. USA* **2007**, *104*, 7916–7921.
- [43] A. S. R. Koti, A. P. Wiita, L. Dougan, E. Uggerud, J. M. Fernandez, *J. Am. Chem. Soc.* **2008**, *130*, 6479–6487.
- [44] A. P. Wiita, S. R. K. Ainaravapu, H. H. Huang, J. M. Fernandez, *Proc. Natl. Acad. Sci. USA* **2006**, *103*, 7222–7227.
- [45] G. I. Bell, *Science* **1978**, *200*, 618–627.
- [46] S. Garcia-Manyes, J. Brujic, J. M. Fernandez, *Biophys. J.* **2007**, *93*, 2436–2446.
- [47] J. M. Fernandez, H. Li, *Science* **2004**, *303*, 1674–1678.
- [48] M. K. Beyer, H. Clausen-Schaumann, *Chem. Rev.* **2005**, *105*, 2921–2948.

- [49] A. P. Wiita, R. Perez-Jimenez, K. A. Walther, F. Graeter, B. J. Berne, A. Holmgren, J. M. Sanchez-Ruiz, J. M. Fernandez, *Nature* **2007**, *450*, 124.
- [50] M. Carrion-Vazquez, A. F. Oberhauser, S. B. Fowler, P. E. Marszalek, S. E. Broedel, J. Clarke, J. M. Fernandez, *Proc. Natl. Acad. Sci. USA* **1999**, *96*, 3694–3699.
- [51] S. Labeit, B. Kolmerer, *Science* **1995**, *270*, 293–296.
- [52] H. B. Li, W. A. Linke, A. F. Oberhauser, M. Carrion-Vazquez, J. G. Kerkvliet, H. Lu, P. E. Marszalek, J. M. Fernandez, *Nature* **2002**, *418*, 998–1002.
- [53] P. E. Marszalek, H. Lu, H. B. Li, M. Carrion-Vazquez, A. F. Oberhauser, K. Schulten, J. M. Fernandez, *Nature* **1999**, *402*, 100–103.
- [54] H. Lu, B. Isralewitz, A. Krammer, V. Vogel, K. Schulten, *Biophys. J.* **1998**, *75*, 662–671.
- [55] H. Lu, K. Schulten, *Chem. Phys.* **1999**, *247*, 141–153.
- [56] H. Lu, K. Schulten, *Biophys. J.* **2000**, *79*, 51–65.
- [57] T. Ackbarow, X. Chen, S. Keten, M. J. Buehler, *Proc. Natl. Acad. Sci. USA* **2007**, *104*, 16410–16415.
- [58] T. Erdmann, U. S. Schwarz, *Phys. Rev. Lett.* **2004**, *92*, 108102–108104.
- [59] E. Evans, K. Ritchie, *Biophys. J.* **1997**, *72*, 1541–1555.
- [60] S. Keten, M. J. Buehler, *Phys. Rev. Lett.* **2008**, *100*, 198301–198304.
- [61] S. Keten, M. J. Buehler, *Nano Lett.* **2008**, *8*, 743–748.
- [62] R. Merkel, P. Nassoy, A. Leung, K. Ritchie, E. Evans, *Nature* **1999**, *397*, 50–53.
- [63] S. Improtta, A. S. Politou, A. Pastore, *Structure* **1996**, *4*, 323–337.
- [64] J. Brujic, R. I. Hermans, K. A. Walther, J. M. Fernandez, *Nat. Phys.* **2006**, *2*, 282–286.
- [65] J. Brujic, R. I. Z. Hermans, S. Garcia-Manyes, K. A. Walther, J. M. Fernandez, *Biophys. J.* **2007**, *92*, 2896–2903.
- [66] A. S. R. Koti, H. H. Huang, A. P. Wiita, H. Lu, K. A. Walther, M. Carrion-Vazquez, H. Li, J. M. Fernandez, *Biophys. J.* **2007**, *92*, 225–233.
- [67] B. Efron, *The Jackknife, the Bootstrap, and Other Resampling Plans*, Society for Industrial and Applied Mathematics, Philadelphia, **1982**.
- [68] H. B. Li, M. Carrion-Vazquez, A. F. Oberhauser, P. E. Marszalek, J. M. Fernandez, *Nat. Struct. Biol.* **2000**, *7*, 1117–1120.
- [69] G. S. Hammond, *J. Am. Chem. Soc.* **1955**, *77*, 334–338.
- [70] K. A. Dill, S. Bromberg, K. Z. Yue, K. M. Fiebig, D. P. Yee, P. D. Thomas, H. S. Chan, *Protein Sci.* **1995**, *4*, 561–602.
- [71] J. N. Onuchic, P. G. Wolynes, *Curr. Opin. Struct. Biol.* **2004**, *14*, 70–75.
- [72] A. Sali, E. Shakhnovich, M. Karplus, *Nature* **1994**, *369*, 248–251.
- [73] P. G. Wolynes, *Q. Rev. Biophys.* **2005**, *38*, 405–410.
- [74] C. Tanford, *Science* **1978**, *200*, 1012–1018.
- [75] P. A. Fernandes, M. J. Ramos, *Chem. Eur. J.* **2004**, *10*, 257–266.
- [76] D. Marx, M. E. Tuckerman, J. Hutter, M. Parrinello, *Nature* **1999**, *397*, 601–604.
- [77] A. Staib, D. Borgis, J. T. Hynes, *J. Chem. Phys.* **1995**, *102*, 2487–2505.
- [78] M. E. Tuckerman, K. Laasonen, M. Sprik, M. Parrinello, *J. Phys. Condens. Matter* **1994**, *6*, A93–a100.
- [79] M. E. Tuckerman, D. Marx, M. Parrinello, *Nature* **2002**, *417*, 925–929.
- [80] B. K. Carpenter, *Determination of Organic Reaction Mechanisms*, Wiley, New York, **1984**.
- [81] F. A. Carey, R. J. Sundberg, *Advanced Organic Chemistry*, Plenum, New York, **1990**.
- [82] J. R. Grigera, *J. Chem. Phys.* **2001**, *114*, 8064–8067.
- [83] T. E. Wales, J. R. Engen, *Mass Spectrom. Rev.* **2006**, *25*, 158–170.
- [84] W. Humphrey, A. Dalke, K. Schulten, *J. Mol. Graph.* **1996**, *14*, 33–38.
- [85] M. T. Nelson, W. Humphrey, A. Gursoy, A. Dalke, L. V. Kale, R. D. Skeel, K. Schulten, *Int. J. Supercomput. Appl. High Perform. Comput.* **1996**, *10*, 251–268.

Received: August 30, 2008

Published online on December 4, 2008